Journal of the Korean Physical Society, Vol. 66, No. 2, January 2015, pp. 229∼233

Tower-like ZnO Nanorods Synthesized by Using a Hydrothermal Process

Ju Hyun Kim, Mu Sung Lee and Hyon Chol Kang*
Department of Materials Science and Engineering, Chosun University, Gwangju 501-759, Korea

(Received 7 October 2014, in final form 6 November 2014)

We report the effect of growth temperature on the characteristics of Zinc oxide (ZnO) nanorods (NRs) synthesized by using a hydrothermal process. As the temperature was increased in the range of 70 − 200 °C, the diameter of the ZnO NRs varied from 20 to 45 nm, which might be associated with the fusing process. The samples grown at temperatures greater than 150 °C exhibited tower-like tips originating from repeated secondary anisotropic growth to minimize the surface energy by eliminating the polar (002) planes. We also observed that a secondary anisotropic growth occurred simultaneously, with no disturbance of the atomic arrangement, and that the diameters of the tower-like NRs converged to approximately 20 nm.

PACS numbers: 61.46.Km, 81.05.Dz, 81.07.Gf, 68.37.Lp
Keywords: ZnO, Tower-like nanorods, Anisotropic growth, Structural properties, Raman spectroscopy
DOI: 10.3938/jkps.66.229

I. INTRODUCTION

Zinc oxide (ZnO) has been widely investigated because it has unique properties such as a wide bandgap of 3.37 eV and a large exciton binding energy of 60 meV at room temperature (RT) [1, 2]. In particular, one-dimensional ZnO nanostructures such as nanorods (NRs) and nanowires have received considerable attention due to their importance in basic science and technological applications for electronic and opto-electronic devices. In order to synthesize ZnO NRs, various fabrication methods such as the hydrothermal process, pulse laser deposition, and vapor phase transport deposition have been developed [3–8]. Among them, the hydrothermal process has many advantages, such as its low cost, the simplicity of the procedure, its applicability to large areas, etc. Many studies on the controlled growth of ZnO NRs by varying the experimental parameters have been reported, and the physical properties of ZnO NRs as functions of their dimensions have been extensively investigated [5,9–13]. ZnO NRs of approximately 100 nm in diameter can be easily fabricated by using the hydrothermal process whereas reports on the synthesis of ZnO NRs as small as 30 nm in diameter are quite rare. This might be attributed to the poor mechanical stability of NRs with a high aspect ratio, *i.e.*, the ratio of diameter to length. ZnO NRs with a smaller diameter tend to bend during the early stage of growth and then fuse with neighboring NRs to form larger NRs, the so-called fusing process [5, 13–15]. The fusing process is well known to depend extensively on the growth conditions, such as the growth temperature and the concentration of reaction species [5, 13–15].

In this study, the effect of growth temperature on the characteristics of ZnO NRs during the hydrothermal process was investigated. ZnO NRs with diameters ranging from 20 to 45 nm were synthesized and characterized. We found that the fusing process was facilitated as the temperature increased, leading to an increase in the most probable diameter of the NRs. Repeated secondary anisotropic growth near the tips was also observed with samples grown at temperatures greater than 150 °C, resulting in the formation of tower-like ZnO NRs.

II. EXPERIMENTS

Zinc-acetate-dihydrate [$Zn(CH_3COO)_2{\cdot}2H_2O$, Sigma Aldrich] powder was dissolved in deionized water under stirring to form an aqueous solution with a concentration of 0.05 M at RT. Because the pH value is one of the key parameters for determining the characteristics of the resulting ZnO samples, it was set to pH = 9 in the present study, at which ZnO was grown in the form of NRs with very good uniformity in diameter and length. Ammonium hydroxide (NH_4OH) was then added to obtain an alkaline environment. Prior to the hydrothermal process, a seed layer on a sapphire(001) substrate was prepared at 250 °C for 20 min, in which the zinc acetate dilydrate/ammonium hydroxide solution, diluted to 0.005 M, was used to disperse the seeds uniformly. The samples were then subjected to the hydrothermal process in an autoclave. To examine the effect of growth temperature on the properties of the NRs, we prepared five samples

*E-mail: kanghc@chosun.ac.kr; Fax: +82-62-230-7311

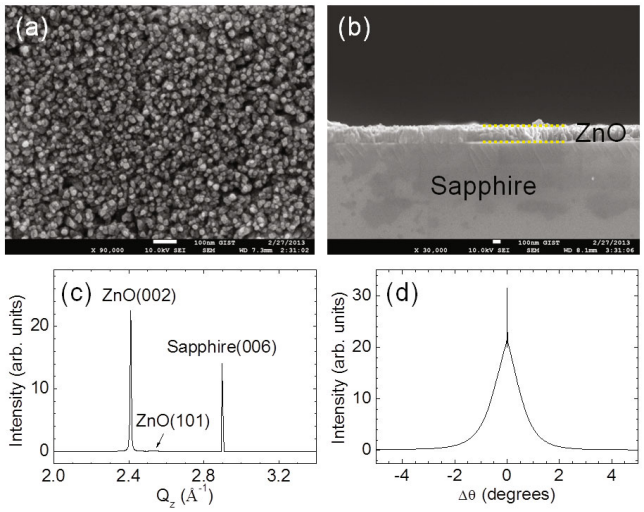

Fig. 1. (Color online) (a) Top-view and (b) cross-sectional SEM images of the sample grown at 50 °C. (c) $\theta - 2\theta$ scan profile and (d) θ-rocking curve measured at the (002) Bragg peak. The FWHM of the sharp component in the rocking curve is 0.015°.

at ambient temperatures of 50, 70, 100, 150, and 200 °C. The samples were kept at the desired temperatures for 2 hours and then cooled naturally to RT. All of the results presented in this study were reproducible.

The crystalline structure of the as-grown samples was characterized by using synchrotron X-ray diffraction (XRD) measurements at the 5D beamline of the Pohang Light Source. A typical powder XRD pattern ($\theta - 2\theta$ scan) was measured. The morphologies of the samples were examined using field-emission scanning electron microscopy (SEM, Hitachi S-4700). The atomic structure of individual ZnO NRs was examined using transmission electron microscopy (TEM, Tecnai F20, operated at 200 keV) performed at Korea Basic Science Institute (KBSI) Gwangju Center. Finally, the optical properties were investigated using micro-Raman spectroscopy (LabRamHR, Jobin Yvon). An Ar ion laser (wavelength = 514.5 nm) was used as an excitation source. An input power of approximately 10 mW at the sample position was used.

III. RESULTS AND DISCUSSION

We first discuss the characteristics of the sample grown at 50 °C. Figures 1(a) and (b) show top-view and cross-sectional SEM images of the sample, respectively. Clearly, the surface is mainly covered by nanometer-scale grains. The size of the grains is quite uniform, and a mean value of ∼17 nm was obtained by averaging the sizes of 200 grains. ZnO with a columnar structure approximately 240 nm thick was observed in the cross-sectional SEM image. Although the columns were separated, it was unclear from the SEM image whether ZnO was grown in the form of NRs or thin films.

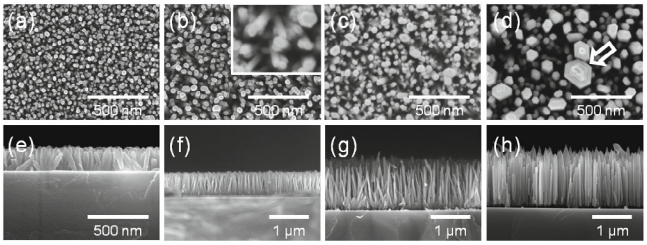

Fig. 2. (a−d) Top-view and (e−h) cross-sectional SEM images of the ZnO NRs grown at 70, 100, 150, and 200 °C, respectively. A fusing process is highlighted in the inset of (b). The arrow in (d) indicates the multiple steps representing the repeated secondary anisotropic growth.

To clarify the structure of the ZnO sample grown at 50 °C, we analyzed the XRD patterns. Shown in Fig. 1(c) is the $\theta - 2\theta$ scan profile. With a sapphire (006) peak for the substrates, an intense peak at $Q_z = 2.41$ Å^{-1} was detected, which was assigned as the (002) Bragg peak of wurtzite ZnO. The sharp peak implies that the sample is highly crystalline. Note that a weak (101) Bragg peak at $Q_z = 2.53$ Å^{-1} was also observed. Figure 1(d) shows the θ-rocking curve measured at the ZnO (002) peak. The full width at half maximum (FWHM) is approximately 0.015°. This indicates that the (002) planes of ZnO are highly ordered along the substrate's normal direction and that the mosaic structure is remarkably small. We note that the weak broad profile of the rocking curve with a FWHM value of approximately 1.2 could originate from the disordered structure of ZnO. This is also good enough to ensure preferred growth with a (002) orientation. A two-component line shape of the rocking curve has often been observed in high-quality ZnO thin films [16]. Therefore, the XRD results suggest that ZnO grown at 50 °C is in the form of a thin film composed of columnar structures rather than NRs. This sample is seen to have been grown epitaxially to the sapphire substrates, which is confirmed by the azimuthal angle scan of the off-specular Bragg reflections (data not shown).

Figure 2 presents typical top-view [(a)−(d)] and cross-sectional [(e)−(h)] SEM images of the ZnO samples grown at 70, 100, 150, and 200 °C, respectively. The images illustrate evidently well-defined NR arrays. The hexagonal NRs, mostly clearly shown in Fig. 2(d), featured flat basal planes that were mostly oriented perpendicular to the substrates' surfaces. The growth of ZnO NRs can be explained by using a classical model based on anisotropic growth during the hydrothermal process [5,10,17], in which the growth rate of the (001) planes is somewhat faster than that of the lateral (101) and (100) planes. Proper seed layers also contributed to the growth of NRs by providing nucleation sites on a nanometer scale [18,19]. We note that all samples exhibited preferential (002) planes in the direction normal to the surface in the XRD profiles (data not shown), similar to the $\theta - 2\theta$ scan

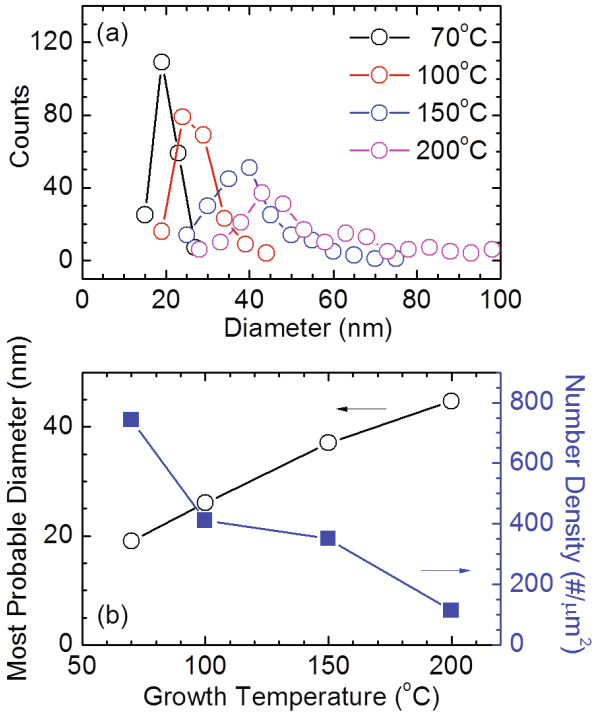

Fig. 3. (Color online) (a) Diameter distributions of ZnO NRs grown at 70, 100, 150, and 200 °C. Each data set was obtained from 200 NRs. (b) Plots of the most probable diameters and the number density as functions of the growth temperature.

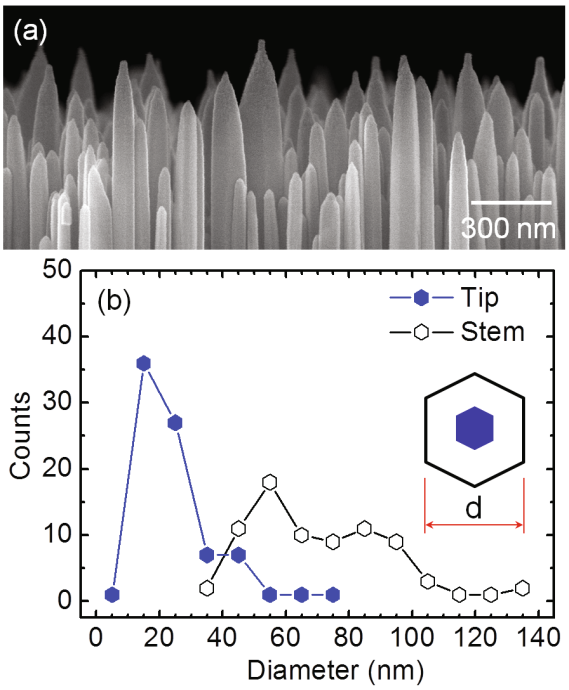

Fig. 4. (Color online) (a) Cross-sectional SEM image taken from the sample grown at 200 °C. This confirms the growth of tower-like ZnO NRs. (b) Diameter distributions of both the host stem and the tip in individual tower-like NRs. The data show that the diameters of the tips in the tower-like NRs converge to approximately 20 nm by repeated secondary anisotropic growth. The inset shows a schematic illustration of the diameter of the ZnO NR stem and tip.

profile shown in Fig. 1(c).

The top-view SEM images shown in Fig. 2 reveal that the diameter and the number density of the ZnO NRs drastically changed with increasing growth temperature. In Fig. 3(a), we present the diameter distribution of ZnO NRs. The data were obtained by analyzing 200 NRs. The number density, defined as the number of NRs per μm^2, decreased from ∼741 to ∼113 in the temperature range of 70 − 200 °C. In addition, the diameter distribution of the NRs narrowed and showed a simple Gaussian profile for samples grown at lower temperatures. The most probable diameters were estimated to be approximately 20, 26.5, 37.7, and 45 nm at 70, 100, 150, and 200 °C, respectively, as plotted in Fig. 3(b). The dependence of the most probable diameter on the growth temperature can be explained by the fusing process, as highlighted by the inset of Fig. 2(b). The fusing process originates from the disturbance of the capillary force between NRs as they became longer and closer to each other, resulting in bundling of NRs to form larger ones [20, 21]. Fusing was facilitated as the growth temperature increased. Moreover, multiple steps near the tips, as indicated by an arrow in Fig. 2(d), were observed clearly for samples grown at 150 and 200 °C. Note that the electrostatic force induced by the piezoelectric characteristic of ZnO NRs might also be a possible origin; however, a further investigation is required.

Shown in Fig. 4(a) is a cross-sectional SEM image taken from the sample grown at 200 °C. The figure shows a continuous decrease of the diameter with each step. This observation suggests that secondary anisotropic growth was repeated and changed the tip shape to form tower-like NRs. Typically, multiple steps are associated with the repeated formation of layered structures with hexagonal basal planes, which has been observed in tower-like ZnO NRs synthesized by using the vapor transport method [22–25].

The synthesis of tower-like ZnO NRs can be rationalized in terms of the competition between axial and lateral growth. In other words, the total surface energy can be minimized spontaneously by eliminating the polar (002) planes, leading to a large growth rate in the polar (001) direction as compared with the non-polar (101) and (100) directions. One may postulate that the association and dehydration of complex molecules such as Zn^{2+}, OH^-, $[Zn(NH_3)_4]^{2+}$, and $[Zn(OH)_4]^{2-}$ at the growing interface between the precursor solution (mostly solvents) and the NR tip are associated with the change in the growth rates for the axial and the lateral directions, resulting in a repeated secondary anisotropic growth of NRs [24, 26]. The repeated formation of two-dimensional discs on the growing front of the hexagonal stems is thought

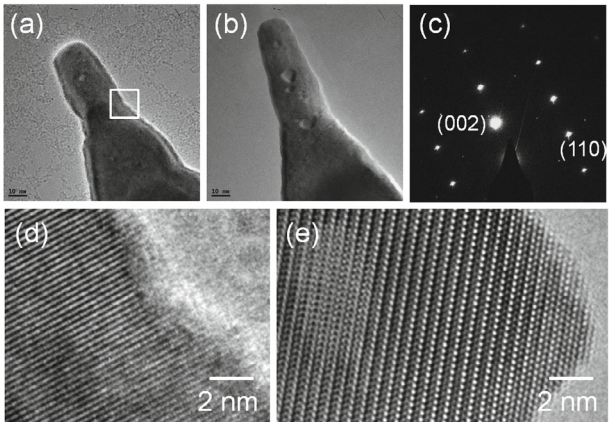

Fig. 5. (a),(b) TEM images of individual tower-like ZnO NRs. (c) Selected-area electron diffraction patterns of the ZnO NR in (a), suggesting that the tower-like ZnO NR is single-crystal wurtzite ZnO. (d) High-resolution TEM image taken from the region marked by a box in (a). No significant atomic inhomogeneities are observed. (e) High-resolution TEM image shows that the atomic sequence is perfect from tip to stem, without stacking faults or twins.

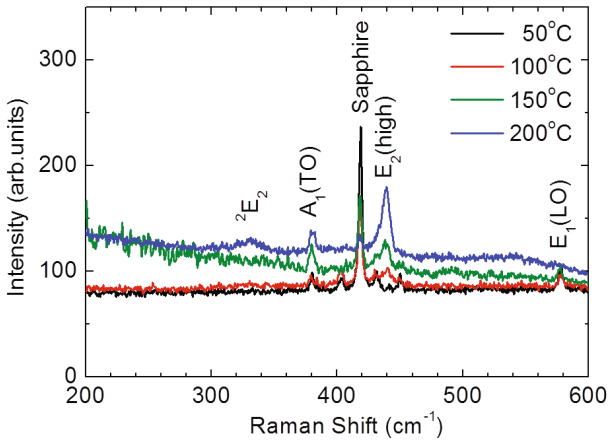

Fig. 6. (Color online) Micro-Raman spectra of ZnO NRs with different growth temperatures. The E_2 (high) mode is shown to be intensified with increasing growth temperature.

to be a plausible mechanism. This is confirmed by the presence of multiple steps near the tips. In addition, such anisotropic growth results in a significant decrease in the diameter of a single NR by a factor of more than 5, as shown in Fig. 4(a). We analyzed the diameter distribution of 80 tower-like NRs from the sample grown at 200 °C, and the results are presented in Fig. 4(b). The inset is a schematic of the measured diameters of tower-like NRs. The diameters of the stems were dispersed widely from 30 to 145 nm whereas those of the tips converged to approximately 20 nm. This might be an equilibrium value constrained by the surface energies between polar and non-polar surfaces under the present growth conditions.

We investigated the atomic structure of individual tower-like NRs by using TEM, and high-resolution images near the tips of the NRs are shown in Fig. 5. The NRs are single crystals, as confirmed by the well-defined electron diffraction patterns shown in Fig. 5(c). All diffraction spots are assigned to wurtzite ZnO. As explained above, the straight stems of the NRs were modified into tower-like tips. Figure 5(d) shows a high-resolution TEM image of the atomic structure at the region of interest (near the step) indicated by a box in Fig. 5(a). The interplanar distance was measured to be 0.26 nm, corresponding to the distance between the (002) planes of wurtzite ZnO. Although the growth behavior of the NRs was changed at the steps, there are no remarkable structural inhomogeneities such as stacking faults or twins. In particular, the atomic stacking sequence is perfect from the tip to the straight stem, with no stacking faults or strained layers, as shown in Fig. 5(e). Indeed, we inspected many individual tower-like NRs by using high-resolution TEM; however, no meaningful planar defects at the steps were observed [27,28]. This evidently indicates that the morphological changes to the tower-like tips occurred with no disturbance in the atomic arrangement.

Figure 6 shows the micro-Raman spectra of ZnO samples in the frequency range from 200 to 600 cm^{-1} for different growth temperatures. Note that the intense peak at 418 cm^{-1} arises from the single-crystal sapphire substrate. Six Raman active phonon modes are well known in the wurtzite ZnO crystal [29]. In the present study, the transverse optical (TO) A1 mode, the high-frequency E_2 mode, and the longitudinal optical (LO) E1 mode were clearly detected at 379, 439, and 579 cm^{-1}, respectively. The A_1 and the E_1 modes are associated with the polar orientations, and the E_2 (high) mode arises from the non-polar orientations. From the sample grown at 50 °C, the A_1 and the E_1 peaks are clearly shown whereas no E_2 peak is observed. This is consistent with the XRD results shown in Fig. 1, confirming that the ZnO sample grown at 50 °C was grown in the form of a thin film rather than as NRs. The E_2 mode peak appeared when the growth temperature was increased up to 70 °C, and it increased in intensity with increasing growth temperature, indicating an improving crystallinity of the wurtzite ZnO NRs. In particular, the FWHM of the E_2 mode peak for the sample grown at 200 °C is 9.5 cm^{-1}, indicating that the ZnO NRs are high-quality single crystals, consistent with the TEM results. Note that a weak broad peak at 330 cm^{-1} was also detected, which can be assigned to the second-order optical mode of the E_2 phonon mode ($^2E_2$) [30].

IV. CONCLUSION

The influence of growth temperature on the morphology of ZnO NRs synthesized by using the hydrothermal

process was investigated. ZnO NRs aligned perpendicular to the substrates were synthesized. We found that the growth temperature in the hydrothermal process was a key experimental parameter for controlling the diameter of the ZnO NRs. Furthermore, at temperatures greater than 150 °C, tower-like ZnO NRs were observed. This was attributed to repeated secondary anisotropic growth, which minimized the surface energy. We will perform further investigations of one-pot synthesis of metal nanoparticles attached to ZnO NRs by using the hydrothermal process, in which the optical properties can be greatly improved via surface plasmonic effects.

ACKNOWLEDGMENTS

This study was supported by research funds from Chosun University (2014).

REFERENCES

[1] D. C. Look, B. Claflin, Ya. I. Alivov and S. J. Park, Phys. Stat. Sol. (a) **201**, 2203 (2004).
[2] U. Ozgur, Y. I. Alivov, C. Liu, A. Teke, M. A. Reshchikov, S. Dogan, V. Avrutin, S-J. Cho and H. Morkoc, J. Appl. Phys. **98**, 141301 (2005).
[3] T. Pauporté, D. Lincot, B. Viana and F. Pellé, Appl. Phys. Lett. **89**, 233112 (2006).
[4] M. H. Huang, Y. Wu, H. Feick, N. Tran, E. Weber and P. Yang, Adv. Mater. **13**, 113 (2001).
[5] L. E. Greene, M. Law, J. Goldberger, F. Kim, J. C. Jhonson, Y. Zhang, R. J. Saykally and P. Yang, Angew. Chem. Int. Ed. **42**, 3031 (2003).
[6] Y. Zhang, R. E. Russo and S. S. Mao, Appl. Phys. Lett. **87**, 133115 (2005).
[7] C. H. Ahn, S. K. Mohanta, N. E. Lee and H. K. Cho, Appl. Phys. Lett. **94**, 261904 (2009).
[8] Y. Li, G. Duan, G. Liu and W. Cai, Chem. Soc. Rev. **42**, 3614 (2013).
[9] H. M. Chen *et al.*, ACS Nano **6**, 7362 (2012).
[10] J. X. Wang, X. W. Sun, Y. Yang, H. Huang, Y. C. Lee, O. K. Tan and L. Vayssieres, Nanotechnology **17**, 4995 (2006).
[11] H. Hu, X. Huang, C. Deng, X. Chen and Y. Qian, Mater. Chem. Phys. **106**, 58 (2007).
[12] M. C. Akgun, Y. E. Kalay and H. E. Unalan, J. Mater. Res. **27**, 1445 (2012).
[13] C. Xu and D. Gao, J. Phys. Chem. C 116, 7236 (2012).
[14] H. Zhitao, L. Sisi, C. Kinkui and C. Yong, J. Semicond. **34**, 063002 (2013).
[15] J. M. Wu, Y.-R. Chen and Y.-H. Lin, Nanoscale **3**, 1053 (2011).
[16] S. I. Park, T. S. Cho, S. J. Doh, J. L. Lee and J. H. Je, Appl. Phys. Lett. **77**, 349 (2000).
[17] N. Wang, Y. Cai and R. Q. Zhang, Mater. Sci. Eng. R **60**, 1 (2008).
[18] S. Baruah and J. Dutta, J. Sol-Gel. Sci. Technol. **50**, 456 (2009).
[19] D. Y. Kim, S.-O. Kim, M. S. Kim, K. G. Yim. J.-Y. Leem, S. Kim and D.-Y. Lee, J. Korean Phys. Soc. **60**, 94 (2012).
[20] X. Zhou, Y. Zhou, J. C. Ku, C. Zhang and C. A. Mirkin, ACS Nano **8**, 1511 (2014).
[21] M. K. Dawood, H. Zheng, N. A. Kurniawan, K. C. Leong, Y. L Foo, R. Rajagopalan, S. A. Khan and W. K. Choi, Soft Matter **8**, 3549 (2012).
[22] P. Hu, Y. Liu, X. Wang, L. Fu and D. Zhu, Chem. Commun. 1304 (2003).
[23] D. Deng, S. T. Martin and S. Ramanathan, Nanoscale **2**, 2685 (2010).
[24] Y. Yan, X. Wang, H. Chen, L. Zhou, X. Cao and J. Zhang, J. Phys. D: Appl. Phys. **46**, 155304 (2013).
[25] Z. Zhang *et al.*, J. Phys. Chem. B **110**, 8566 (2006).
[26] Z. Wang, X. Qian, J. Yin and Z. Zhu, J. Solid State Chem. **177**, 2144 (2004).
[27] L. Xu. Y. Su, Y. Chen, H. Xiao, L. Zhu, Q. Zhou and S. Li, J. Phys. Chem. B **110**, 6637 (2006).
[28] Y. Dai, Y. Zhang, Y. Q. Bai and Z. L. Wang, Chem. Phys. Lett. **375**, 96 (2003).
[29] T. C. Damen, S. P. S. Porto and B. Tell, Phys. Rev. **142**, 570 (1966).
[30] N. Xu, Y. Cui, Z. Hu, W. Yu, J. Sun, N. Xu and J. Wu, Opt. Exp. **20**, 14857 (2012).